Arthropod Structure & Development 45 (2016) 475–487

Contents lists available at ScienceDirect

Arthropod Structure & Development

journal homepage: www.elsevier.com/locate/asd

Distribution of the obligate endosymbiont *Blochmannia floridanus* and expression analysis of putative immune genes in ovaries of the carpenter ant *Camponotus floridanus*

Maria Kupper [a, *], Christian Stigloher [b], Heike Feldhaar [c], Roy Gross [a]

[a] Department of Microbiology, Biocentre, University of Würzburg, Am Hubland, D-97074 Würzburg, Germany
[b] Division of Electron Microscopy, Biocentre, University of Würzburg, Am Hubland, D-97074 Würzburg, Germany
[c] Department of Animal Ecology I, Bayreuth Center of Ecology and Environmental Research (BayCEER), University of Bayreuth, D-95440 Bayreuth, Germany

ARTICLE INFO

Article history:
Received 23 March 2016
Received in revised form
15 September 2016
Accepted 19 September 2016
Available online 6 October 2016

Keywords:
Primary endosymbiont
Oogenesis
Transovarial transmission
Insects
Hymenoptera

ABSTRACT

The bacterial endosymbiont *Blochmannia floridanus* of the carpenter ant *Camponotus floridanus* contributes to its hosts' ontogeny via nutritional upgrading during metamorphosis. This primary endosymbiosis is essential for both partners and vertical transmission of the endosymbionts is guaranteed by bacterial infestation of oocytes. Here we present a detailed analysis of the presence and localisation of *B. floridanus* in the ants' ovaries obtained by FISH and TEM analyses. The most apical part of the germarium harbouring germ-line stem cells (GSCs) is not infected by the bacteria. The bacteria are detectable for the first time in lower parts of the germarium when cystocytes undergo the 4th and 5th division and *B. floridanus* infects somatic cells lying under the basal lamina surrounding the ovarioles. With the beginning of cystocyte differentiation, the endosymbionts are exclusively transported from follicle cells into the growing oocytes. This infestation of the oocytes by bacteria very likely involves exocytosis–endocytosis processes between follicle cells and the oocytes. Nurse cells were never found to harbour the endosymbionts. Furthermore we present first gene expression data in *C. floridanus* ovaries. These data indicate a modulation of immune gene expression which may facilitate tolerance towards the endosymbionts and thus may contribute to their transovarial transmission.

1. Introduction

Insects are by far the most diverse and a highly successful animal group on earth, which is reflected not only in species richness and abundance but also in the variety of ecosystems they inhabit. Diversification and evolutionary success of insects are at least partially facilitated by symbiotic associations with microorganisms (Buchner, 1965). Bacterial endosymbionts may contribute to their hosts' biology in various ways (Feldhaar, 2011), e.g. via nutritional upgrading of unbalanced diets (Nogge, 1981; Zientz et al., 2004), enhanced resistance to pathogens or parasitoids and thermal tolerance (Dunbar et al., 2007; Kaltenpoth, 2009; Oliver et al., 2010). These host associated bacteria comprise so-called primary and secondary endosymbionts. The latter are facultative symbionts from the host's perspective and are found intracellularly and/or extracellularly in various host tissues (Dale and Moran, 2006). Secondary endosymbionts can be transmitted vertically or horizontally (Oliver et al., 2010; Russell et al., 2003).

In contrast, primary endosymbionts have obligate associations with their insect hosts that developed over long evolutionary timescales. Generally these bacteria are endowed with small genomes (<1 Mb) (Klasson and Andersson, 2010; McCutcheon and Moran, 2012). Accordingly, primary endosymbionts have lost the ability to multiply independently from their hosts (Baumann, 2005; Feldhaar and Gross, 2009). The localisation of primary endosymbionts within their insect hosts is most frequently restricted to specialised cells, the so-called bacteriocytes, which often form multicellular symbiotic organs called bacteriomes (Buchner, 1965). Due to the obligate nature of the association, primary endosymbionts are transmitted strictly vertically.

Though the transmission of primary endosymbionts occurs strictly vertically, transmission routes of different endosymbionts may be highly diverse. Host biology (ovipary vs. vivipary) and localisation of endosymbionts in their host have selected different

* Corresponding author.
E-mail addresses: maria.kupper@freenet.de (M. Kupper), christian.stigloher@uni-wuerzburg.de (C. Stigloher), feldhaar@uni-bayreuth.de (H. Feldhaar), roy@biozentrum.uni-wuerzburg.de (R. Gross).

http://dx.doi.org/10.1016/j.asd.2016.09.004

transmission routes of endosymbiotic bacteria to the host's offspring. The viviparous tsetse fly harbours one primary and several secondary endosymbionts that are also transmitted vertically. The primary endosymbiont *Wigglesworthia glossinida* as well as the secondary endosymbiont *Sodalis glossinidius* are transmitted to the developing embryo via milk gland secretions. Remarkably, in the milk gland secretions *W. glossinidia* has an extracellular localisation. The secondary endosymbiont *Wolbachia* already infects trophocytes and developing oocytes (Balmand et al., 2013). The transmission of the primary endosymbiont of aphids, *Buchnera*, proceeds also including an extracellular stage. Within the parthenogenetic and viviparous aphids *Buchnera* is transmitted from maternal bacteriocytes into blastulae (early embryos) through a series of exo- and endocytotic processes (Koga et al., 2012).

Whilst the transmission of endosymbionts is most often established late during development of eggs and embryos in viviparous insects, the infection of oocytes during transovarial transmission in oviparous insects occurs either early or late during oogenesis. For example, the endosymbionts *Schneideria nysicola* of seed bugs of the genus *Nysius* (Hemiptera) are generally localised intracellularly in a pair of large bacteriomes which are in close association with the gonads. In adult female bugs *S. nysicola* was also found in the "infection zone" in the middle of each germarium, where the first egg-chamber forms within the telotrophic-meroistic ovarioles of the seed bugs. Within the "infection zone" the *Schneideria* endosymbionts preferentially localised in the ovarial bacteriocytes. Additionally, *S. nysicola* was observed in the "symbiont balls" at the anterior poles of each oocyte, suggesting that the endosymbionts enter the developing oocytes ensuring vertical transmission of the bacteria (Matsuura et al., 2012a, 2012b). In the scale insect *Marchalina hellenica*, an early infection of germ cells, the so-called cystocytes, was suggested. As a consequence both cell types deriving from the cystocytes, the trophocytes and oocytes, are infected with bacterial endosymbionts. During oogenesis, the endosymbionts are progressively transported from trophocytes into the developing oocyte (Szklarzewicz et al., 2013). Apart from such cases of very early infection of oocytes with bacterial endosymbionts there are several cases showing infection of oocytes through nurse cells in later stages of oogenesis or even early embryos. For example, it was shown that *Wolbachia* in chalcid wasps of the genus *Aphytis* are transmitted from the nurse cells into developing oocytes through cytoplasmic bridges between the two cell types (Zchori-Fein et al., 1998). The bacterial endosymbiont *Westeberhardia cardiocondylae* of the invasive ant *Cardiocondyla obscurior* is located in nurse cells and transmitted into late-stage oocytes during nurse cell depletion (Klein et al., 2016). The bacterial endosymbionts of the leafhopper *Macrosteles laevis*, which were located in a structure called "symbiotic ball" in the perivitelline space between the oolemma and the follicular epithelium, invade the oocyte at the posterior pole only after the end of oocyte growth (Kobialka et al., 2015).

The symbioses between bacteria of the genus *Blochmannia* and carpenter ants of the genus *Camponotus* was the first endosymbiosis between bacteria and animals ever described (Blochmann, 1882; Buchner, 1965). *Blochmannia floridanus* resides free within the cytoplasm of bacteriocytes in the midgut tissue as well as in matured oocytes of *Camponotus floridanus* (Blochmann, 1882; Sauer et al., 2002; Schröder et al., 1996). The bacteria upgrade the diet of their insect hosts (Feldhaar et al., 2007; Gil et al., 2003). During metamorphosis of the ants the numbers of bacteria and of bacteriocytes in the midgut increase dramatically and peak in the late pupal stage, transforming the entire midgut tissue into a huge symbiotic organ. Subsequently, in adult animals the number of bacteriocytes and, concomitantly, of *Blochmannia* continuously decrease, since the symbiosis is apparently of less relevance for older animals (Stoll et al., 2010). Interestingly, during the period of bacterial proliferation in the pupal stages two negative immune-regulators, the peptidoglycan recognition proteins PGRP-LB and PGRP-SC2 are highly expressed only in the midgut suggesting a down-modulation of the immune response possibly contributing to symbiont tolerance within the midgut tissue (Ratzka et al., 2013).

Blochmann (1882), Buchner (1918) as well as Hecht (1923) focussed on the localisation of the bacteria (previously also called "Blochmann bodies", (Koch, 1960)) mainly during embryogenesis of *Camponotus ligniperdus*. The bacteria were found in the developing bacteriocytes within the determined midgut tissue within embryos, but also in cells which come into close contact with the predestined ovarian tissue during embryogenesis (Hecht, 1923). However, very young oocytes were not found to be infected with the endosymbionts, while developing oocytes in fertile animals were described to become infected via follicle cells (Blochmann, 1882; Buchner, 1918). Recent analyses showed that oocytes in posterior parts of the ovarioles of *C. floridanus* are the only cells infected by the endosymbionts (Sauer et al., 2002; Schröder et al., 1996).

To date, the understanding of the mechanism of transovarial transmission of *Blochmannia* remained limited. Thus, in the present manuscript we investigated the localisation of *B. floridanus* in ovaries of queenless *C. floridanus* workers during oogenesis based on imaging techniques using fluorescent *in situ* hybridisation (FISH) and transmission electron microscopy (TEM). In addition, we present first expression data of immune-related genes in the ovarian tissue possibly contributing to endosymbiont control or tolerance.

2. Material and methods

2.1. Ants

C. floridanus colonies C90 (derived from a mated queen from Florida, Orchid Island, 2001) and C152 (derived from a mated queen from Florida, Orchid Island, 2002) were maintained in a climatic chamber at 25 °C, 70% humidity and a 12 h light–dark cycle. Animals were fed twice to three times a week with cockroaches and honey water (50% w/w). Workers normally have small and underdeveloped ovaries. However, when workers are isolated from their colonies, in the absence of a fertile queen and queen-laid eggs they activate oocyte development and begin to lay haploid eggs after several weeks (Endler et al., 2004). Therefore, orphaned (queenless) workers could be used for our investigations after two to four months. Respective sub-colonies consisted of 60–80 major workers and at least 200 minor workers. To maintain nursing behaviour of workers, larvae (at least stage L2) and pupae (stages P1-P3) with stages defined according to Stoll et al., 2010 were provided.

2.2. Fluorescent in situ hybridisation (FISH)

For analysing the distribution of *B. floridanus* in worker ovaries FISH was performed as previously described (Feldhaar et al., 2007). Endosymbionts were visualised with a probe Bfl172 targeting a specific region of the *B. floridanus* 16S rRNA (5′-CCTATCTGGGTTCATCCAATGGCATAAGGC-3′). Oligonucleotides were labelled with the fluorophore Alexa488 by the manufacturer (Sigma–Aldrich Chemie GmbH, Munich, Germany). The respective sense probe Bfl172sense (5′-GCCTTATGCCATTGGATGAACCCAGATAGG-3′) was used as a negative control for specificity.

Ovaries of workers were dissected in ice-cold PBS (pH7.4). Ovaries with at least one matured egg at the posterior end were transferred in small glass vials for fixation in 4% (w/v) paraformaldehyde in PBS. After 2 h of fixation at room temperature (RT) the fixative was exchanged by PBS by three 5 min washes. Then samples were

dehydrated by incubation in 30%, 50%, 70%, 90% and two times in 100% ethanol each time 3–5 min. Hybridisation was performed in hybridisation buffer (35% formamide, 900 mM NaCl, 20 mM Tris/HCl pH 7.5, 0.2% SDS) with 500 mM of each oligonucleotide probe. Samples were placed in a humid chamber and incubated for 2–3 h at 46 °C in the dark. After hybridisation, the samples were washed for 30 min in washing buffer (70 mM NaCl, 20 mM Tris/HCl pH 7.5, 5 mM EDTA, 0.01% SDS) at 48 °C. In addition, DAPI was supplied to the wash buffer for counter staining of eukaryotic and bacterial DNA. Subsequently samples were rinsed in sterile distilled water, placed on microscopy slides, mounted in Mowiol 4-88 (Carl Roth, Karlsruhe, Germany) and analysed by confocal laser scanning microscopy (CLSM) with a Leica TCS SP5 (Leica Microsystems, Wetzlar, Germany). Pictures were taken with LAS AF version 2.7.3.9723 (Leica) and further processed using ImageJ 1.49v and Adobe Illustrator CS4 14.0.0.

2.3. Sample preparation for transmission electron microscopy (TEM) and electron tomography

Ovaries of workers were dissected in ice-cold PBS, separated from surrounding fat body tissue and transferred into Karnovsky's fixative (2% paraformaldehyde, 2.5% glutaraldehyde in 0.1M PBS, pH 7.4) and left at 4 °C for overnight fixation. Samples were washed five times each 5 min in cacodylic acid buffer (50 mM cacodylic acid, pH 7.2) and post-fixed on ice in 2% osmium tetroxide in 50 mM cacodylic acid buffer for 2h. After five times washing in dH_2O samples were stained in 0.5% uranyl acetate overnight at 4 °C. Then the samples were dehydrated in an increasing ethanol series (30 min each in 50, 70, 90% and two times in 100% ethanol at 4 °C; two times 30 min in 100% ethanol at room temperature) and incubated three times for 30 min each in propylene oxide. Propylene oxide was gradually exchanged by Epon812 and samples were allowed to polymerize in Epon812 for at least 48 h at 60 °C. Sectioning was performed with an Leica EM UC7 ultramicrotome (Leica) and ultra-thin sections (60–100 nm) for TEM or semi-thin sections for tomography (200–250 nm) were post-stained for 20 min in 2% uranyl acetate in ethanol and for 10 min in Reynold's lead citrate (Reynolds, 1963) to increase contrast. Additionally, grids holding sections for tomography were carbon coated.

2.4. TEM and electron tomography

The prepared sections were analysed using a 200 kV JEM-2100 (Jeol, Munich, Germany) transmission electron microscope equipped with a TemCam F416 4k x 4k camera (Tietz Video and Imaging Processing Systems, Gauting, Germany). Electron micrographs of standard sections were taken with EMMenu 4.0.9.31 software (Tietz) and further analysed using ImageJ 1.49v with TrakEM2 and arranged using Inkscape 0.91 and Adobe Illustrator CS4 14.0.0. The tilt series for tomogram generation were recorded from at least −65° to +65° with 1° increments with SerialEM (Mastronarde, 2005). The picture series were further processed with eTOMO, a tool within the software package IMOD v4.7 (Kremer et al., 1996).

2.5. Total RNA isolation and quantitative RT-PCR

Total RNA was isolated separately from dissected ovaries, from midguts and from residual bodies (head and thorax) as a control tissue without symbionts. Also, the fat body was not included in residual body samples in order to avoid the detection of constitutive immune gene expressed in the immune organ of the ants. To obtain comparable amounts of tissue 10 ovaries or 15 midguts or 3 residual bodies were dissected on ice in sterile, RNase-free 1x PBS and pooled. Total RNA was extracted using TRIzol® Reagent (Sigma–Aldrich) and purified through RNeasy mini kit columns (Qiagen, Hilden, Germany) including an on-column DNase digestion (RNase-Free DNase Set, Qiagen). Extraction and purification were performed according to the manufacturer's protocols and RNA quality was determined with a Nanodrop® spectrophotometer (Thermo Scientific, Wilmington, DE, USA). In addition, RNA was checked by PCR for contamination with genomic DNA. For each sample cDNA was produced by reverse transcription from 1 μg of total RNA using the RevertAid First Strand cDNA Synthesis Kit (Fermentas). Resulting cDNA was diluted to a final concentration of 10 ng/μl.

For gene expression studies by qRT-PCR oligonucleotide pairs were designed with Primer3 v. 0.4.0 (Koressaar and Remm, 2007; Untergasser et al., 2012). The estimated product size should be 120–140bp with T_m values for each primer pair around 56 °C (Supplementary Table S1). The qRT-PCR experiments were performed on a StepOnePlus™ Real-Time PCR System (Applied Biosystems, Life Technologies GmbH, Darmstadt, Germany) with PCR samples containing 1x Absolute™ PerfeCTa™ SYBR® Green FastMix™ (Rox) (Quanta Biosciences, Gaithersburg, MD, USA), gene-specific oligonucleotides (250 nM each), 1 μl of the cDNA and water to a final volume of 20 μl. Initial enzyme activation for 5 min at 95 °C was followed by 45 cycles of 5 s denaturation at 95 °C, 10 s of annealing at 56 °C and 20 s of extension at 60 °C. Fragment specificity was tested in melting curves and each biological sample was run in triplicate in the qRT-PCR. Results were averaged and relative transcription levels were calculated by the ddCt method (Livak and Schmittgen, 2001) using the housekeeping gene coding for ribosomal protein L32 (*rpL32*, GenBank Acc. No.: EFN68969) as reference.

2.6. Statistical analysis of qRT-PCR results

Statistical analysis was performed using Statistica 64 v12. Expression data were tested for normality between samples with the Shapiro–Wilk W Test (Supplementary Table S2). The average gene expression levels relative to the constitutively expressed housekeeping gene *rpL32* (dCt = Ct(target) − Ct(rpL32)) of six independent samples (six biological replicates as groups of workers taken from queenless sub-colonies, respectively three replicates were either originated from the colony C90 or C152) were determined for three different tissues (residual body, midgut and ovary). Expression levels were tested with an ANOVA in order to investigate the significance of two influencing effects namely “tissue” and “colony” (Supplementary Table S3). Tissue was included as fixed factor in the analyses and nested within colony. Since workers derived from two different original colonies, “colony” was included as random factor. A LSD post hoc test was performed to investigate significant differences of dCt-values between samples (Supplementary Table S4).

3. Results and discussion

3.1. FISH on C. floridanus ovaries: B. floridanus during oogenesis of its host

The distribution of *B. floridanus* in queenless *C. floridanus* worker ovaries was investigated over the course of oogenesis by direct labelling of the endosymbionts with 16S rRNA specific probes in whole-mount FISH experiments.

The germarium is located at the proximal tip of each ovariole (Fig. 1A) and contains the germ-line stem cells (GSCs) in close contact with the terminal filament (TF) cells. Additionally, cystoblasts (CB) and cystocytes, the GSCs' progeny, can be found in the

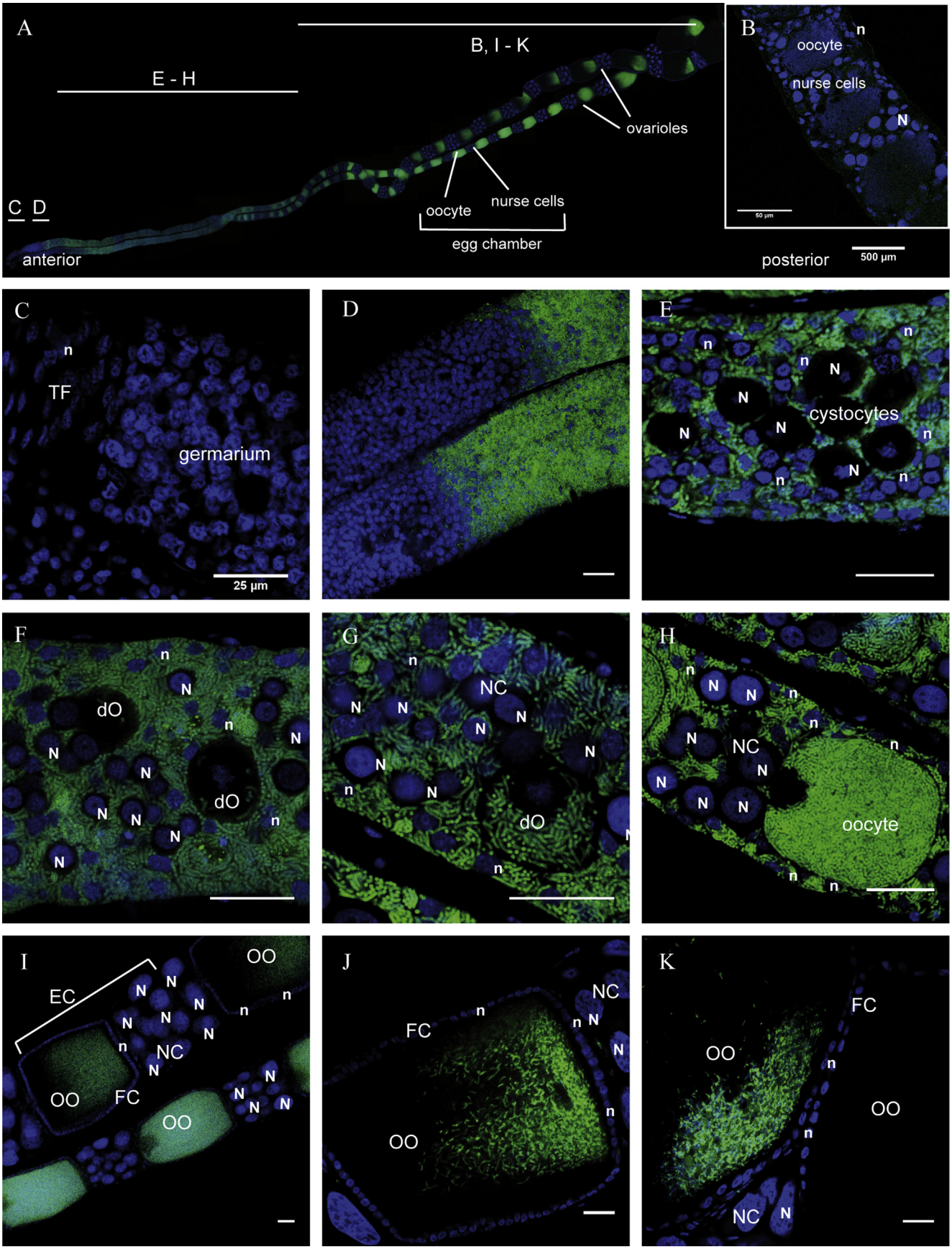

Fig. 1. Distribution of *B. floridanus* during germ cell development and oogenesis in the ant *C. floridanus*. Green colour marks *B. floridanus* detected via FISH probe Bflo172 and blue colour marks nuclei stained with DAPI. All views are oriented from left to right following the anterior–posterior axis. **A**. The overview represents the general structure of two

germarium (Khila and Abouheif, 2008). Our observations show that the most apical part of the germarium is a *Blochmannia*-free segment of the ovariole (Fig. 1C). To confirm these observations a 3D reconstruction of a Z-stack of pictures of the germarium was compiled (Fig. 2A; Supplementary Movie M1). We could not detect any Bfl172-positive fluorescence demonstrating the absence of *B. floridanus* in this part of the germarium.

Supplementary video related to this article can be found at http://dx.doi.org/10.1016/j.asd.2016.09.004.

In lower parts of the germarium the cystoblasts and cystocytes undergo several divisions forming 2-cell, 4-cell, 8-cell and later 16-cell cysts. Each division leads to the shifting of older cysts towards the vitellarium when the younger and more apically located cysts are formed. Between the 4th and the 5th division, they reach the segment where *B. floridanus* is detected quite suddenly (Fig. 1D). The 3-D reconstruction of this segment (Fig. 2B, Supplementary Movie M2) reveals the beginning infection with *B. floridanus* in the periphery of each ovariole. In the beginning only cells lying under the ovariolar epithelial sheath are infected. However, the infection progresses incrementally, though quite rapidly to the interior of the germarium. The bacterial endosymbionts spread into the whole tissue within a region of approximately 100 μm width of the ovariole's proximal-distal axis (Supplementary Fig. S1).

Supplementary video related to this article can be found at http://dx.doi.org/10.1016/j.asd.2016.09.004.

The ovariole's region following this primary “infection zone” is massively infected with the endosymbiont. However, the cytoplasm of cystocytes constituting 16-cell cysts which lie at the beginning of the “infection zone”, as well as the cytoplasm of cystocytes forming 32-cell cysts within the “infection zone” appear to be free from *B. floridanus* (Fig. 1E). After the 5th division the cystocytes of the 32-cell cysts differentiate and one cystocyte grows faster than the other cystocytes eventually becoming the determined oocyte (dO), while the other cystocytes (pro-trophocytes) develop into nurse cells. The dO accompanied by somatic follicular cells is shifted towards the middle of the ovariolar tube and already has the size of at least six nurse cells. At this stage we can detect scattered *B. floridanus* in the cytoplasm of the determined oocyte for the first time (Fig. 1F). Similarly, in 1918 Buchner described the initial infection of follicle cells in *C. ligniperdus* occurring after the formation of accessory nuclei when the oocyte begins to grow. Thus, an early oocyte infection appears to be a general phenomenon in ants of the genus *Camponotus*. (Blochmann, 1882; Buchner, 1918).

During progressing differentiation of nurse cells (NC), oocytes and follicle cells (Fig. 1F–H) we observe not only an increasing number of *B. floridanus* in the dOs which develop into oocytes, but also an infection of the whole ovarian tissue as Bfl172 signals can be found surrounding all nuclei. However, based on CLSM it is not possible to distinguish between the cell types mentioned above and to unravel which cell type is infected. Nevertheless, with the emergence of clearly visible egg chambers, which consist of a NC package followed by an oocyte (OO) which is surrounded by a thin epithelium of small follicle cells (FC), *B. floridanus* was only detected in the growing oocytes (Figs. 1I and 2C, Supplementary Movie M3). In the negative control using the sense probe Bflo172sense no signal could be detected and bacteria were only stained by DAPI (Fig. 1B), thus proving the specificity of the positive probe Bflo172. The periodical alternation of bacteria filled oocytes and bacteria free NC packages results in a necklace-like appearance of the ovarioles (Fig. 1A). Finally, with the end of oocyte growth the endosymbionts seem to migrate towards the posterior pole of the oocyte (Fig. 1I–K). In contrast to the situation in young and growing oocytes when the bacteria are distributed over the entire cytoplasm, high numbers of *B. floridanus* were detected only at the posterior pole of fully grown oocytes (Fig. 1K).

Supplementary video related to this article can be found at http://dx.doi.org/10.1016/j.asd.2016.09.004.

3.2. Determining the distribution of *B. floridanus* in ovaries during oogenesis using TEM

3.2.1. The germarium and the “infection zone”

The TEM data confirm that neither the terminal filament nor the apical part of the germarium and, therefore, the GSCs are infected with *B. floridanus* (Fig. 3A). The GSCs display large nuclei and the cytoplasm contains noticeable mitochondria but no bacteria (Fig. 3B). Additionally, cystoblasts, the immediate progeny of GSCs (Fig. 3C), as well as smaller cells, lying under the basal lamina surrounding the ovariole (Fig. 3C, marked with asterisks), are not infected with *Blochmannia*.

However, in the lower segment of the germarium containing 16-cell and 32-cell cysts we observe *B. floridanus* in cells of the outer layer of the ovariole directly lying under the basal lamina, which confirms our results obtained by FISH (Fig. 4A). In this segment of the “infection zone” cystocytes, which already differentiated into pro-trophocytes and pro-oocytes, can be easily distinguished from other cells due to their dark cytoplasm and the large nuclei. Here, the endosymbionts are located in small and slender cells close to the peritoneal sheet. The rod-shaped bacteria are up to 1 μm wide and show variable length of up to 3 μm as well as the characteristic Gram-negative cell wall structure (Fig. 4C). They reside free within the cytoplasm, but also in vacuole-like structures of these small cells (Fig. 4B). Interestingly, the pro-oocyte (p-O) shows first signs of differentiation since it already is twice as large as the other cells differentiating from cystocytes, the pro-trophocytes, which will develop into nurse cells (Fig. 4A). Nevertheless, we could not observe an infection of pro-oocytes (p-O) this early during oogenesis.

3.2.2. The initial infection of determined oocytes

Before entering the vitellarium, when the determined oocytes reach at least four to five times the size of an average pro-trophocyte, we observe *B. floridanus* residing within these

ovarioles and the overall distribution of *B. floridanus* (green). **B**. Representative view of a section of an ovariole stained with the negative control probe Bflo172sense_Alexa488 and DAPI (blue). The sense probe did not detect bacteria residing within the oocytes. **C**. The apical germarium at the anterior tip of each ovariole contains the germ-line stem cells in close contact with the cells of the terminal filament (TF). This segment of the germarium also contains cystoblasts as direct progeny of GSCs. *B. floridanus* was not detected in the apical part of the germarium. **D**. The “infection zone” is located in the lower parts of the germarium where the bacteria “suddenly” appear. *B. floridanus* seems to rapidly infect the whole ovariole's tissue towards posterior. **E**. The cytoplasm of cystocytes forming 16-cell cysts at the anterior beginning of the “infection zone” remains *B. floridanus*-free. **F**. Two determined oocytes (dO) are shown. These dOs differentiate after the 5th division from one of the cystocytes forming the 32-cell cysts. Scattered endosymbionts were detected inside the cytoplasm of dOs, which acquire a position in the centre of the ovariolar tube. **G and H**. Two views representing the ongoing process of egg-chamber formation. The nurse cells (NC) are of germ cell origin and progressively build packages between dOs, which grow rapidly and develop into oocytes. *B. floridanus* can be detected in the dO and oocytes as well as between nurse cells. **I**. Older egg-chambers (EC) consist of clearly separated oocytes (OO) surrounded by a single cell layer of follicle cells (FC) followed by a compact package of nurse cells. The endosymbionts reside within the whole ooplasm at first **(I)** and are then shifted towards the oocytes' posterior pole **(J)**. **K**. In fully grown oocytes *B. floridanus* resides within a small volume at the cell's posterior pole. Scale bar in **A** represents 500 μm, in **B** 50 μm and in **C-K** 25 μm. (N = nucleus of a nurse cell; n = nucleus of cells of somatic origin and follicle cells)

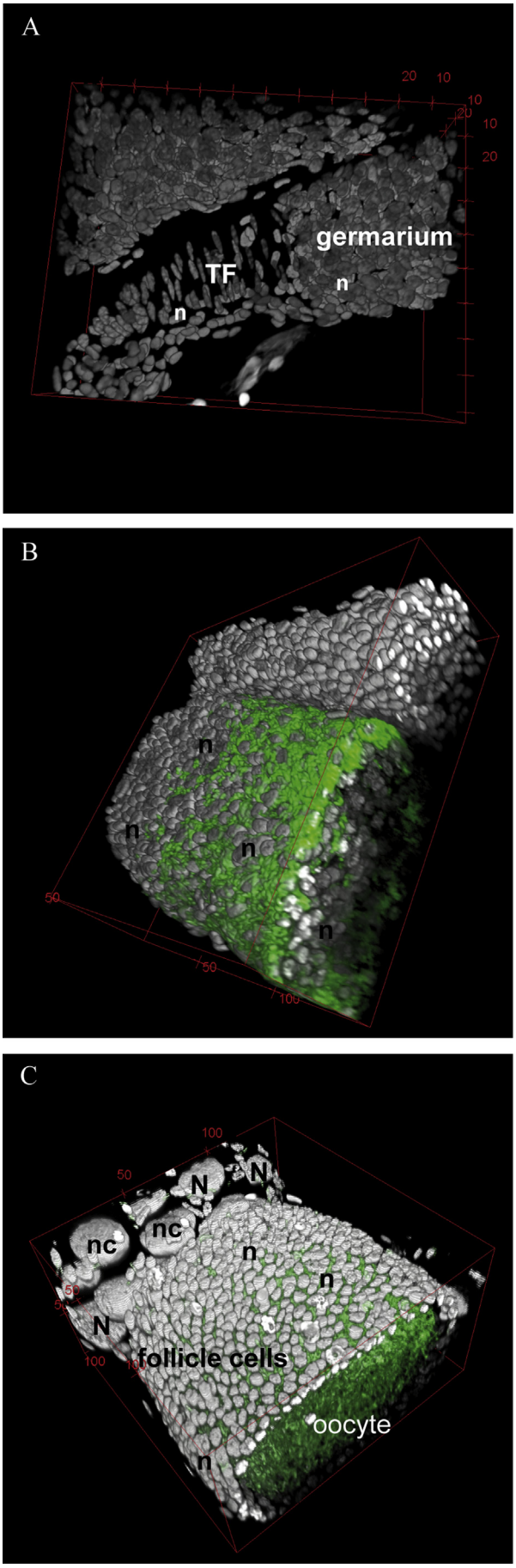

determined oocytes (Fig. 5). The large nuclei of the determined oocytes begin to show an irregular morphology (Fig. 5A) as characteristic accessory nuclei will be generated in the next phase of oogenesis (Fig. 6A). In this particular segment of the ovariole we find the endosymbionts in virtually all cells of somatic origin (CoSO) which will differentiate into follicle cells. As these very young determined oocytes are surrounded by follicle cells, *B. floridanus* can be transmitted over the whole surface of the oocyte rather than at one particular pole. Additionally, it is important to note that the progeny of the GSCs, the cystocytes with nurse cell fate ((pro-)trophocytes) and the determined oocytes, are embedded within the huge mass of *Blochmannia*-filled CoSOs. Astonishingly, the endosymbionts are exclusively transmitted into the determined oocytes but never into the other cystocytes with nurse cell fate. These cells remain uninfected (Fig. 5A). While most of the endosymbionts reside within the cytoplasm of the dO and CoSOs, we also observe some of the bacteria within small vacuole-like structures as shown in Fig. 5B. This phenomenon will be discussed in Section 3.3.

3.2.3. *The infection status of oocytes, nurse cells and follicle cells during egg chamber formation and oocyte growth*

Three major events take place during egg chamber formation in *C. floridanus* ovarioles: (i) the formation of compact nurse cell packages; (ii) the migration of follicle cells to form a thin but closed layer around the oocyte; and (iii) the advancing transmission of *B. floridanus* into the enclosed oocyte.

At the beginning of nurse cell package formation (Fig. 6) there are still long, stretched but slender cells interspersed among the nurse cells (Fig. 6A and B). In contrast to the nurse cells these cells of somatic origin harbour the bacterial endosymbionts. Additionally, cells of the same origin, which are beginning to arrange around the oocyte, are infected with *B. floridanus* (Fig. 6C). The oocytes exhibit the typical accessory nuclei (for further details see e.g. Jaglarz et al. (2008)) which are arranged around the oocyte's large nucleus (Fig. 6A and D). The endosymbionts reside inside the oocyte's cytoplasm in a scattered manner leaving the larger proportion of the ooplasm bacteria-free (Fig. 6A, D and E).

With progressing nurse cell package formation cells of somatic origin (follicle cells) harbouring *Blochmannia* cannot be found between the nurse cells (Fig. 7A and B). The nurse cells exhibit large nuclei and their cytoplasm, which is filled with mitochondria, appears in a typically darker shade in TEM samples (Fig. 7B). Follicle cells surround the oocyte gradually, separating the latter from the nurse cell packages (Fig. 7A). While the number of *B. floridanus* in follicle cells slowly decreases, the oocytes become increasingly packed with the endosymbionts (Fig. 7C and D). With the proceeding transmission of *B. floridanus* into the oocyte, the follicle cells, which finally surround the latter completely, do not harbour endosymbionts anymore, whereas the ooplasm is densely packed with the endosymbionts. This distribution of *Blochmannia*-filled and *Blochmannia*-free ooplasm will change drastically again during further oocyte growth. The 50–100 μm long oocytes packed

Fig. 2. 3-D models of three ovariole segments. Ovarioles were dissected and incubated with the *Blochmannia*-positive probe Bflo172_Alexa488. Nuclei were stained with DAPI. Stacks of single pictures were captured in the z-axis of each sample with a confocal microscope. Stack files were then rendered into 3-D models using the Volume viewer of ImageJ 1.49k and snapshots of the models within the chosen perspective were taken. **A**. The germarium and the terminal filament (TF) of the ovariole are not infected with *B. floridanus*. **B**. A sidewise view into the "infection zone" of the ovariole shows that the infection with *B. floridanus* starts in the outer layers of the tissue. **C**. The majority of the cytoplasmic volume of the oocyte within a young egg-chamber is occupied by *B. floridanus*. Nurse cells (NC) and follicle cells don't harbour the endosymbionts. (N = nucleus of a nurse cell; n = nucleus of cells of somatic origin and follicle cells).

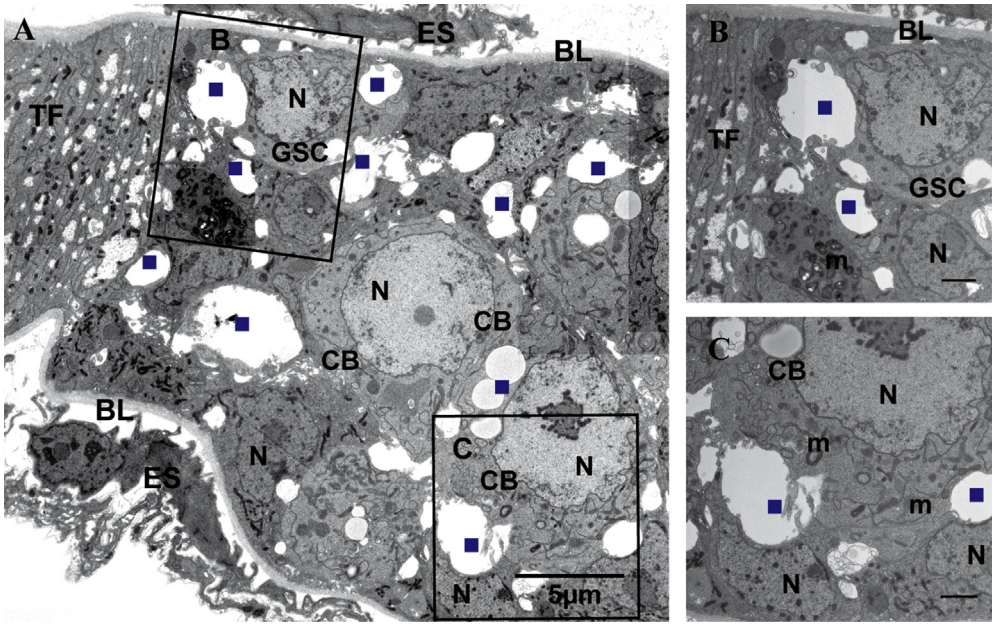

Fig. 3. Electron micrographs presenting the ultrastructure of the apical germarium in *C. floridanus* ovarioles. **A**. Representation of a longitudinal section of the anterior tip of an ovariole showing the terminal filament (TF). Germ-line cell stem cells (GSCs) are in close contact with the TF and the basal lamina (BL) and ovariolar epithelial sheath (ES) surround the ovariole. **B**. Enlargement of a GSC which exhibits a large nucleus (N). The cytoplasm contains mitochondria (m) and appears bacteria-free. **C**. The enlargement shows a cystoblast (CB), the direct progeny of GSCs. Throughout the apical germarium no *B. floridanus* infection was observed. The cytoplasm of GSCs **(A and B)**, of CBs **(C)** and of small somatic cells in the outer layer of the ovariole (marked with asterisks) appear to be free from *B. floridanus*. Holes in the tissue sections which are likely to be artefacts of fixation and Epon embedding are marked with blue squares. Scale bars in **B** and **C** represent 1 µm. (For interpretation of the references to colour in this figure legend, the reader is referred to the web version of this article.)

with *B. floridanus* will grow continuously up to a length of 0.5–1.0 mm (Fig. 1A). An increasing amount of yolk platelets, protein yolk as well as lipid yolk appears in the ooplasm displacing the endosymbionts to the oocyte's posterior pole (Fig. 8).

3.3. Oocyte infection mechanisms: a few observations

In the following we discuss some observations with regard to possible transfer mechanisms of *B. floridanus* into oocytes.

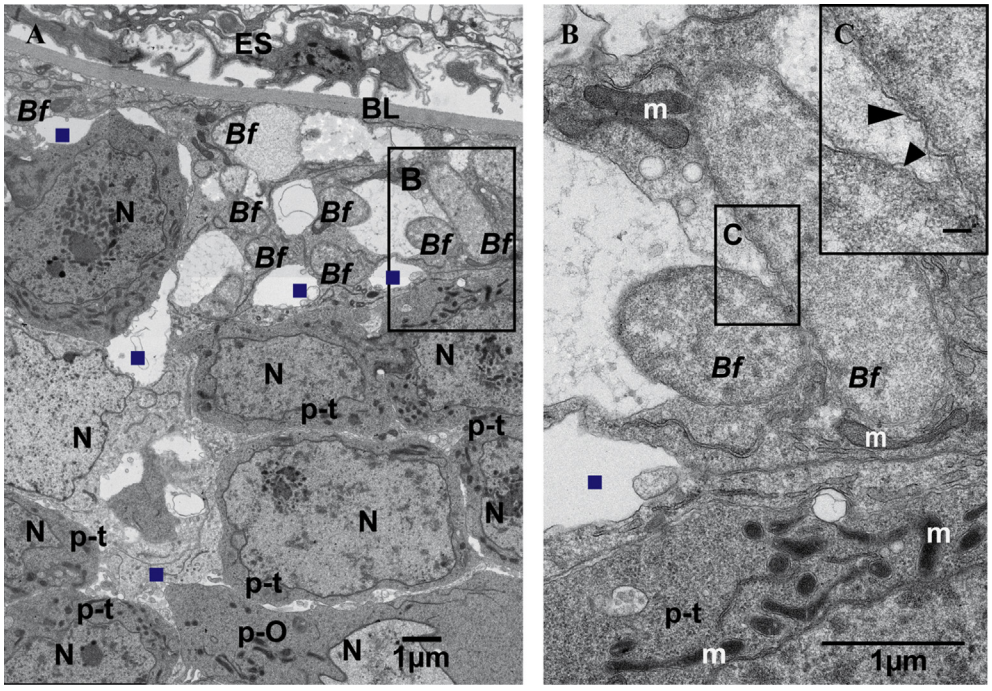

Fig. 4. Electron micrographs showing morphology and ultrastructure of the *C. floridanus* ovariole within the "infection zone" presented in longitudinal sections. **A**. *B. floridanus* (Bf) can be found in small somatic cells lying under the basal lamina (BL), which surrounds each ovariole together with the ovariolar epithelial sheath (ES). Differentiating cystocytes, the pro-trophocytes (p–t) with large nuclei (N) and the pro-oocyte (p-O), remain uninfected, whereas small somatic cells harbour the endosymbionts. **B**. Enlargement of a somatic cell containing Bf and mitochondria (m) in the cytoplasm. **C**. Enlargement of B showing the typical cell wall structure of Gram-negative bacteria (pointed arrowheads). Holes in the tissue sections which are likely to be artefacts of fixation and Epon embedding are marked with blue squares. Scale bar in **C** represents 0.1 µm. (For interpretation of the references to colour in this figure legend, the reader is referred to the web version of this article.)

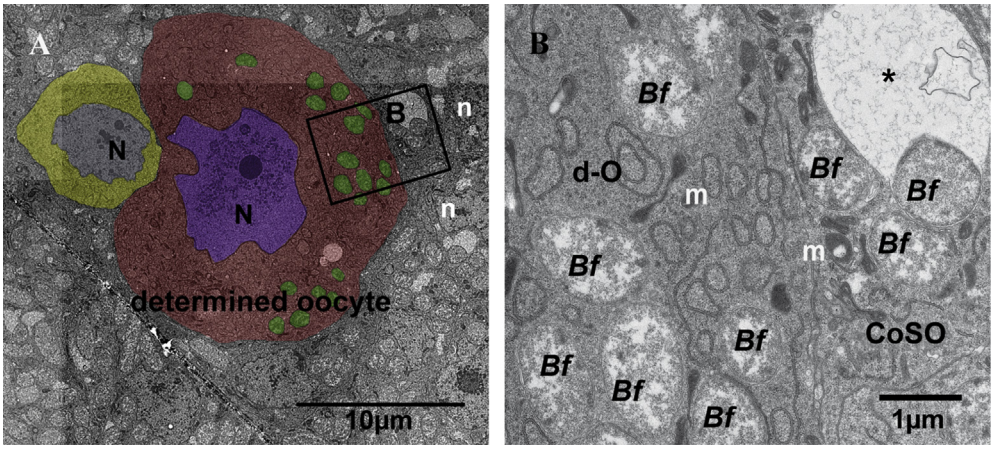

Fig. 5. Ultrastructure of a *Blochmannia* infected determined oocyte presented in electron micrographs of longitudinal sections. **A**. The cytoplasm of the determined oocyte (annotated in red) harbours *B. floridanus* (annotated in green). *B. floridanus* can only be found in the cytoplasm of the determined oocyte and the surrounding follicle cells but not in the nuclei (annotated in purple) or in the cytoplasm of neighbouring nurse cells (cytoplasm annotated in yellow). **B**. Enlargement of A showing mitochondria (m) and *B. floridanus* (Bf) in the ooplasm. Bf also resides within follicle cells which are of somatic origin (CoSO). Whilst most endosymbionts reside free in the cytoplasm, some are surrounded by vacuole-like structures (marked with asterisk). (N = nucleus of a nurse cell or a determined oocyte; n = nucleus of a CoSO)

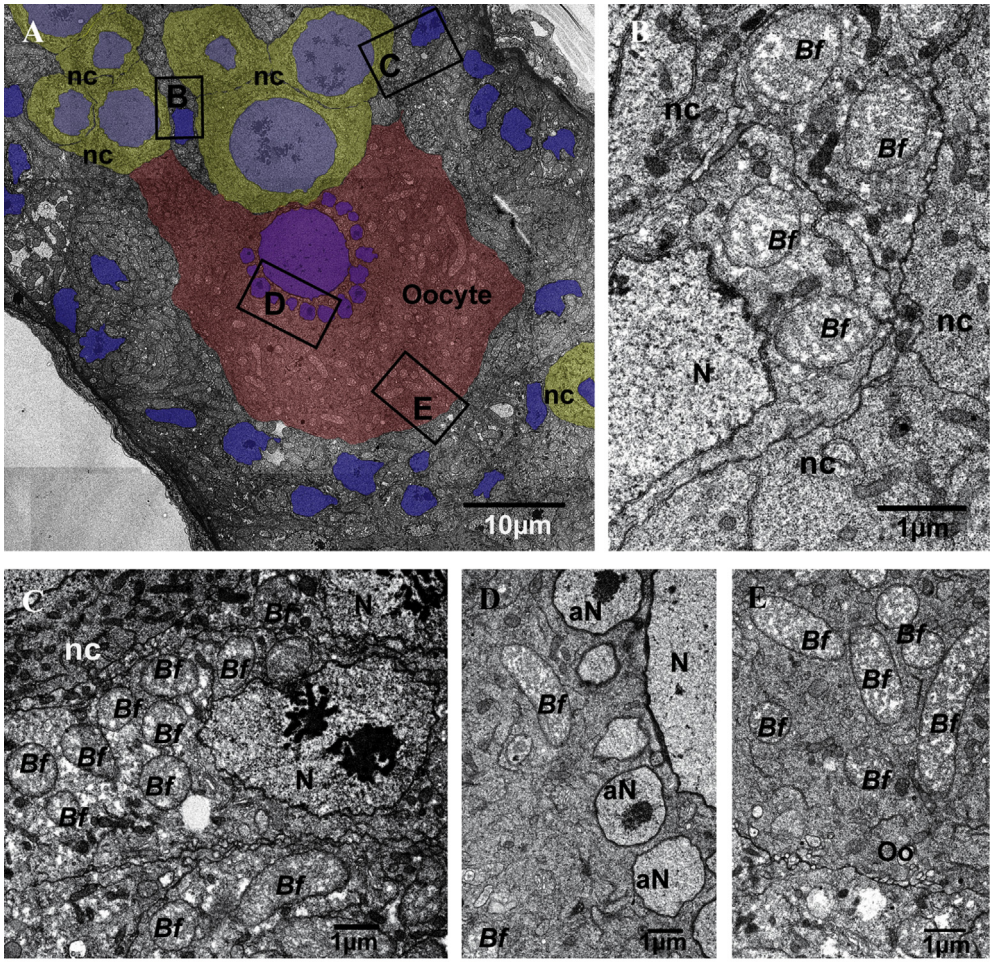

Fig. 6. Electron micrographs of longitudinal sections showing the ultrastructure of an ovariole segment presenting the starting region of egg chamber formation. **A**. The cytoplasm of the oocyte (annotated in red) harbours bacterial endosymbionts whereas there are no bacteria in the nurse cell (nc) cytoplasm (annotated in yellow). Follicle cells (nuclei annotated in blue) are distributed around the oocyte but also between the nurse cells. **B and C**. Enlargement of such a follicle cell between the nurse cells (B) and around the oocyte (C). *B. floridanus* (Bf) resides within their cytoplasm. **D**. Enlargement of A showing the nucleus (N) of the oocyte exhibiting typical accessory nuclei (aN). **E**. Enlargement of A presenting *Blochmannia* in the ooplasm.

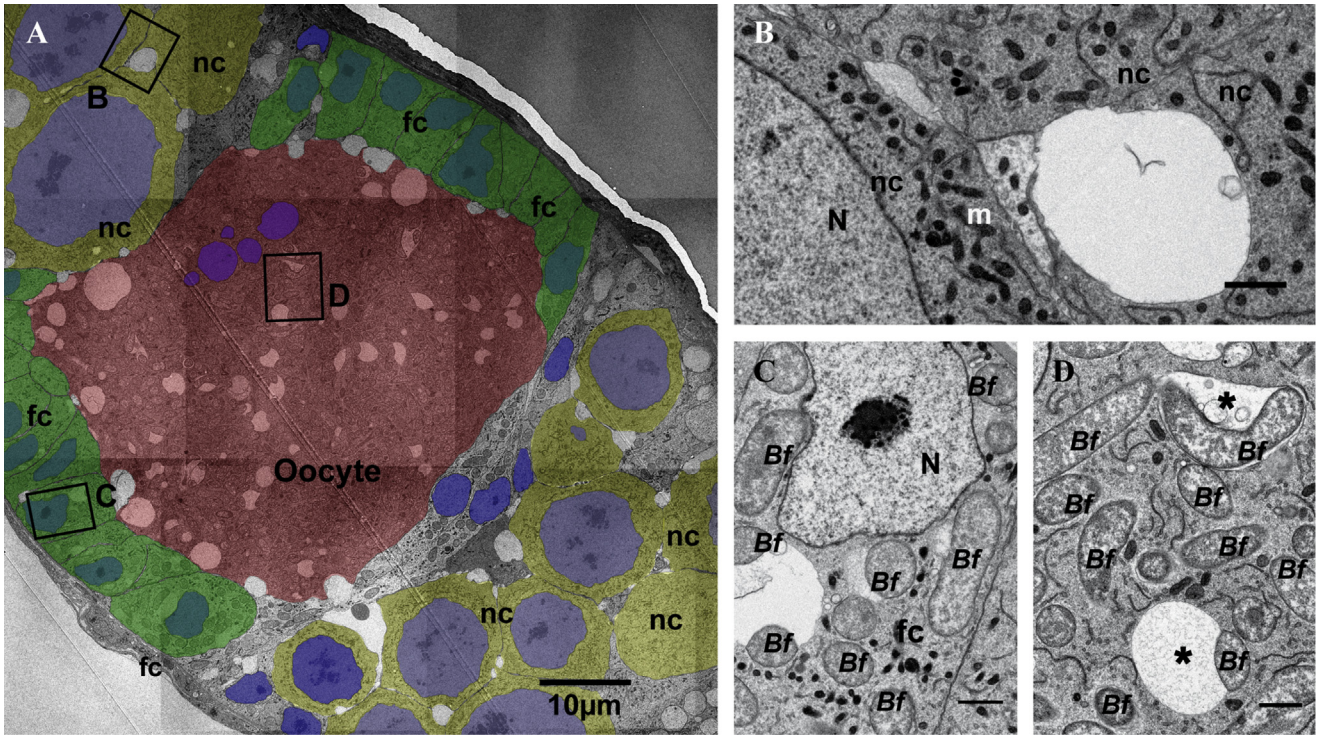

Fig. 7. Electron micrographs presenting the ultrastructure of an egg-chamber of a *C. floridanus* ovariole. **A**. The cytoplasm of the oocyte (annotated in red) harbours bacterial endosymbionts and most of the follicle cells (fc; annotated in green) are distributed in a single cell layer around the oocyte. Nuclei are annotated in blue and the cytoplasm of nurse cells is annotated in yellow. **B**. Enlargement of the nurse cell (nc) package showing the *Blochmannia*-free cytoplasm of nurse cells. **C**. Enlargement of A showing a follicle cell harbouring *B. floridanus* (Bf) in the cytoplasm. **D**. Enlargement of A showing the bacterial endosymbionts residing in the ooplasm or inside of vacuoles (asterisks). Scale bars in **B** - **D** represent 1 µm. (m = mitochondrion; N = nucleus)

Typically, the bacterial endosymbionts reside free within the cytoplasm of oocytes. However, we also find *B. floridanus* inside of vacuole-like structures. Such vacuoles (marked with black asterisks) can already be observed in determined oocytes or cells of somatic origin (CoSO) (Fig. 5), but they increase in number when the endosymbionts are transported into the growing oocytes from the surrounding follicle cells (Figs. 6 and 7). In later stages, when the oocytes are surrounded by follicle cells already cleared from the endosymbionts, bacteria-containing vacuoles in the ooplasm are observed only rarely.

Two types of such bacteria-containing vacuoles can be distinguished. Most of these vacuoles have a single membrane (pointed arrowhead; Fig. 9D, F and G). A tomogram and the respective 3-D model of *B. floridanus* in such a vacuole showed a tight inclusion of the bacteria within the vacuoles (Fig. 9G and H). However, these vacuoles can reach considerable length since more than one bacterium may reside within a single vacuole (Fig. 9H). The second type of vacuole is defined by a double membrane (stealth arrowhead; Fig. 9D and E). In growing oocytes which are not yet fully surrounded by a follicle cell epithelium (Fig. 7) we additionally observe numerous widenings of the intercellular space appearing as invagination-like structures at the cytoplasm membrane between follicle cells and the oocyte (Figs. 7 and 9A–C; marked with red asterisks). In some cases, the vacuoles as well as the invaginations comprise small vesicles (marked with a red square; Fig. 9A–C).

Although our experiments give no further evidence of the precise identity of the described structures, it is likely that they play a role in endosymbiont transfer into oocytes. It is known that some pathogenic bacteria can exploit endocytic pathways in order to access cells thereby avoiding the endosome-to-lysosome pathway and hence avoiding degradation (Asrat et al., 2014; Doherty and McMahon, 2009). According to the genome sequence *B. floridanus* is not endowed with cell invasion factors known from pathogens (Gil et al., 2003). Therefore, it is very likely that the bacterial endosymbionts may be transferred via host endocytosis–exocytosis pathways from follicle cells into the oocytes. The boundary layer between follicle cells and oocytes is known to be a site of extensive cell–cell communication. In the honey bee *Apis mellifera* vitellogenin is exocytosed into the narrow perivitelline space between the follicular epithelium and the oocyte and taken up by the oocyte via endocytosis (Fleig, 1995). Similar events are expected to take place at the follicle cell-oocyte interface in *C. floridanus* ovaries. Consequently, a variety of processes could result in *B. floridanus* being transported into the oocytes. A recent publication focussing on the transmission of *Buchnera* in the pea aphid *Acyrthosiphon pisum* reports the nonselective uptake of the endosymbionts into the developing embryo. The endosymbionts are internalised from the extracellular space by the endocytic activity of the blastula (Koga et al., 2012). Endosymbionts of *Blattella germanica* are released from the bacteriocytes in nymphal instars, cross the ovariole sheath and reside in the extracellular space between the follicle epithelium and the oocyte, where they are in close contact with the oocytes microvilli. Shortly before chorion formation the symbionts are actively phagocytosed by the oocyte (Sacchi et al., 1988). Swiatoniowska et al. (2013) described the transovarial transmission of endosymbionts in two heteropterans, *Nysius ericae* and *Nithecus jacobaeae*. Here, the bacteria are released by the bacteriocytes closely adhering to the oocytes. On the membrane surface of the oocyte the endosymbionts penetrate the ooplasma. While entering the oocyte the bacteria are enclosed by the oocyte's plasma membrane. Therefore, the bacterial endosymbionts of these

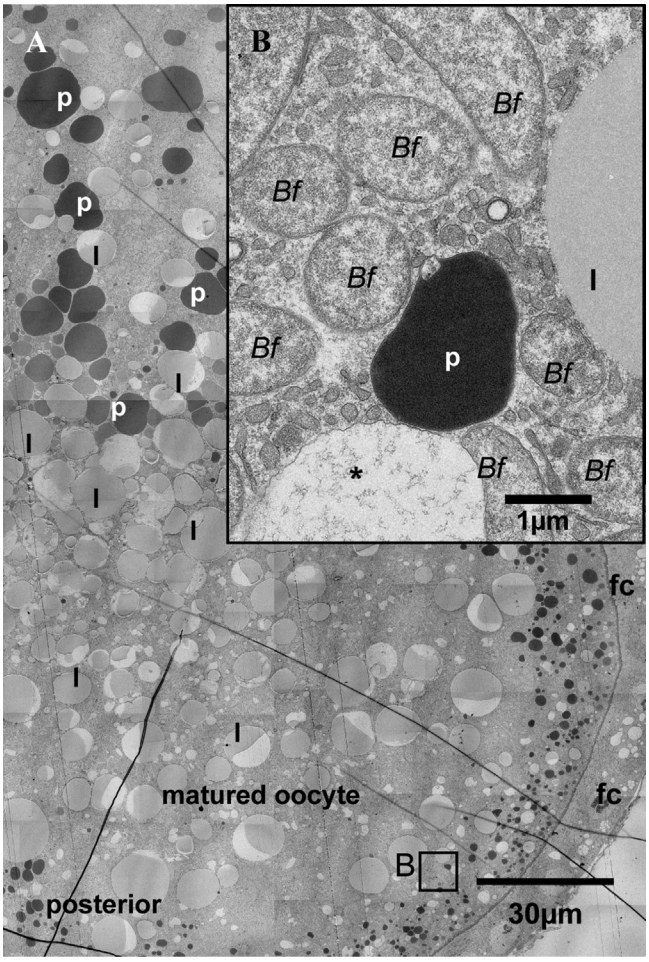

Fig. 8. Electron micrographs presenting the ultrastructure of the posterior pole of a fully grown oocyte in a longitudinal section. **A**. The cytoplasm of the oocyte is filled with yolk platelets (protein yolk (p) and lipid yolk (l)) and follicle cells (fc) surround the oocyte. *B. floridanus* can only be found at the posterior pole of the oocyte. **B**. Enlargement of A showing *B. floridanus* (*Bf*) residing either free in the posterior ooplasm or within vacuole-like structures (marked with asterisk).

Heteroptera reside within the ooplasma surrounded by a host-derived membrane, the so-called perisymbiotic membrane (Swiatoniowska et al., 2013).

It is possible that, similar to the endosymbiont *Buchnera* of the aphid *A. pisum* (Koga et al., 2012), *B. floridanus* may migrate to the follicle cell-oocyte interface to be exocytosed directly into the narrow extracellular space. The endosymbionts would then be taken up by the oocyte either by endocytosis. This would result in *B. floridanus* residing within a single membrane vacuole (Fig. 9D and F). However, this uptake strategy would require an extracellular phase of the endosymbionts, but so far extracellular *Blochmannia* have been detected neither in the midgut nor in the ovaries of the ants.

Another entry strategy could involve a budding-like mechanism as it has been described for the pathogen *Orientia tsutsugamushi* in mites or an actin-based protrusion mechanism as used by human pathogens *Listeria monocytogenes* and *Shigella flexneri* (Hybiske and Stephens, 2008). In this scenario, *B. floridanus* should migrate to the periphery of a follicle cell facing the oocyte and being slowly extruded within a small bud. The outermost layer of such a bud would derive from the follicle cell membrane. The oocyte may take up this bud by endocytosis processes resulting in *B. floridanus* residing within a vacuole with a double membrane (Fig. 9D and E). Alternatively, *B. floridanus* could use the force generated by actin polymerization to protrude from the follicle cell membrane and force engulfment into the neighbouring oocyte, also resulting in a bacteria-containing double-membrane vacuole (Hybiske and Stephens, 2008). A slow and non-phagocytic degradation of the vacuole membranes via the state of single membrane vacuoles would eventually lead to the release of *B. floridanus* into the ooplasm. However, it is also possible that the *Blochmannia*-containing double membrane vacuoles may not be related to bacterial entry, but they may indicate that autophagocytotic processes (Romanelli et al., 2014) may occur in the oocyte (Fig. 9D and E).

3.4. Insights into immune-gene expression in C. floridanus ovarian tissue

Tissue specific differential expression of immune genes strongly suggests an important role of the immune system in the control of endosymbiont multiplication and distribution within insect hosts (Login et al., 2011; Ratzka et al., 2012). In *C. floridanus* it has been shown that its endosymbiont is recognized by the animal's immune system (Ratzka et al., 2011). However, differential expression of so-called pattern recognition receptors (PRRs) recognizing bacterial peptidoglycan (PGN) has been observed in various tissues and developmental stages of the ants (Ratzka et al., 2013). The general function of such PRRs is the recognition of either DAP- or Lys-type peptidoglycan, resulting in the activation of signalling cascades which lead to expression of antimicrobial defence factors (Aggrawal and Silverman, 2007). A special type of PRR, endowed with an amidase activity, recognises and degrades peptidoglycan, thus eliminating the microbial signal. Such amidase-PRRs are considered to be negative regulators of the immune response (Steiner, 2004). In *C. floridanus* these amidase PRRs (PGRP-LB and PGRP-SC2) were shown to be strongly upregulated only in the midgut tissue and only during pupation of the ants. Since this is exactly the period of massive endosymbiont expansion, it was suggested that a down-modulation of immune reactions occurs, which may permit bacterial multiplication and spreading in the midgut tissue during metamorphosis (Ratzka et al., 2013).

For this reason we focussed on analysing the expression of the two *C. floridanus* genes encoding amidase PRRs, PGRP-LB (EFN73971) and PGRP-SC2 (EFN73970), and additionally the gene encoding PGRP-SA (GenBank Acc. No.: EFN70060; previously annotated as PGRP-2), in the ovarian tissue which harbours the endosymbionts. The peptidoglycan recognition protein PGRP-SA is a part of the Toll signalling pathway in *C. floridanus* (Gupta et al., 2015; Michel et al., 2001). Gene expression in the ovaries was compared to gene expression in the midgut and the residual body, devoid of endosymbionts, of queenless workers.

Similar to the results obtained in the midgut during pupal stages, the two PRR genes encoding the negative immune regulators, PGRP-LB and PGRP-SC2, are significantly up-regulated in the ovaries of the workers (Fig. 10; Supplementary Table S3). However, the expression of certain immune genes may vary depending on the colony analysed. In fact, the expression of *PGRP-LB* is significantly induced by the factor "tissue" ($p < 0.0001$) and colony-specific (interaction "tissue*colony" $p = 0.001$; Fig. 10C; Supplementary Table S3). While in colony C90 *PGRP-LB* expression is only 2-fold higher in the ovarian tissue, in colony C152 it is increased 20-fold when compared to gene expression in the residual body. Similarly, in the midgut *PGRP-LB* expression is only 3-fold higher in colony C90, while in colony C152 its expression is 30-fold increased. Nevertheless, the same tendency of *PGRP-LB* gene expression was observed in both colonies. In a previous work it was shown that the expression of three genes encoding antimicrobial

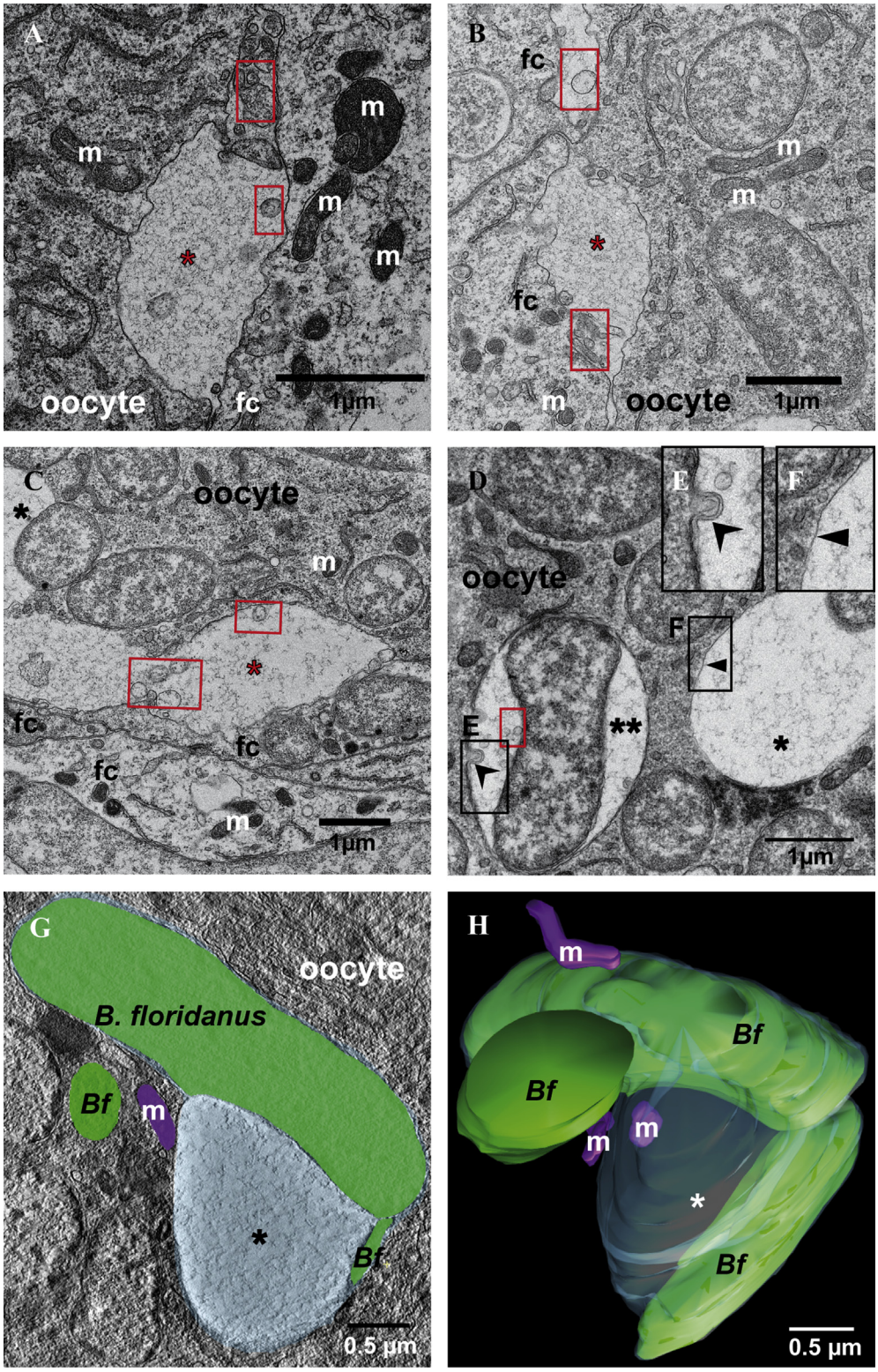

Fig. 9. Infection of oocytes with *B. floridanus*. **A - C**. The electron micrographs show *B. floridanus* residing inside follicle cells and oocytes. Invagination-like structures (red asterisks) appear at the cytoplasmic membrane between the follicle cell (fc) and oocyte. *B. floridanus* resides free in the ooplasm or within vacuoles (black asterisks). **D**. Electron micrographs showing *B. floridanus* residing in the ooplasm as well as in vacuoles exhibiting either a single membrane (single black asterisk, membrane marked with pointed arrowhead) or double membranes (double black asterisks, membrane marked with stealth arrowhead). Red squares mark vesicles within vacuoles and invaginations (A–D). **E and F**. The enlargements present membrane structures of the vacuoles in detail. **G**. A tomogram slice showing *B. floridanus* (green) inside a vacuole (light blue; marked with asterisk). The vacuolar membrane completely surrounds the bacterial endosymbiont. **H**. The 3-D model of the respective structure in G shows *B. floridanus* engulfed in the vacuole. The bacterial cell-wall was annotated in green, the vacuole membrane was annotated in light blue, and mitochondria were annotated in purple. (m = mitochondrion). (For interpretation of the references to colour in this figure legend, the reader is referred to the web version of this article.)

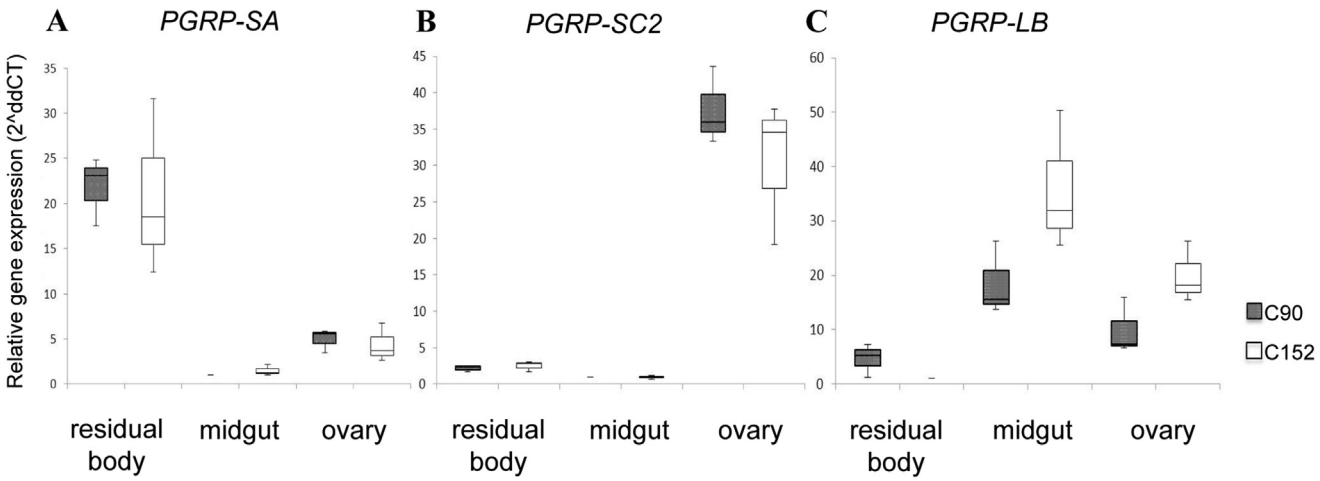

Fig. 10. Expression of immune-related genes in ovary, midgut and residual body of different *C. floridanus* colonies (C90: hatched box; C152: white box). Average gene expression levels relative to the housekeeping gene *rpL32* (dCt = Ct (target) - Ct(rpL32)) of three independent samples each per colony were determined from different tissues. These dCt-values of the genes (**A**) *peptidoglycan recognition protein-SA* (*PGRP-SA*), (**B**) *PGRP-SC2*, and (**C**) *PGRP-LB* were used to create box plots. Box-plots show normalized changes in gene expression relative to the tissue with lowest expression level (2^{-ddCt}-values).

peptides in the bumblebee *Bombus terrestris* shows significant specificity for the host line-parasite pairing, as host lines showed different gene expression patterns upon infection with several *Crithidia bombi* isolates (Riddell et al., 2009). Our results suggest that the down-regulation of the *PGRP-LB* gene expression in the endosymbiont bearing tissues is a specific characteristic for *C. floridanus*; however, the intensity of expression modulation depends on the colony. Interestingly, with an approximately 35-fold increase in expression the *PGRP-SC2* gene is very strongly and about equally expressed in the ovaries of workers derived from both colonies (Fig. 10B; Supplementary Table S3). In contrast, PGRP-SA expression was significantly lower in the midgut and ovary than in the residual body (Fig. 10A). As mentioned above, PGRP-SA activates the Toll pathway (Michel et al., 2001). The down-regulation of expression of this PRR supports the suggested down-modulation of the immune response in the endosymbiont bearing tissue. Taken together, the down-regulation of *PGRP-SA* and the up-regulation of the expression of two genes encoding amidase PRRs in the ovarian tissue of *C. floridanus* may indicate a down-modulation of the initiation of an immune response within the tissue and the reduced immune response in ovarian tissue may support tolerance and transovarial transmission of *B. floridanus* as it was suggested for the tolerance of the endosymbionts in the midgut tissue during metamorphosis (Ratzka et al., 2013).

3.5. Concluding remarks

In this work we characterised the transovarial transmission of the endosymbiont *B. floridanus* during oogenesis of its ant host. Six major attributes of endosymbiont transmission during oogenesis can be noted: (i) the most apical part of the germarium containing germ-line stem cells (GSCs), cystoblasts and early cysts is not infected with the bacterial endosymbionts; (ii) in the lower segment of the germarium with late 16-cell and early 32-cell cysts *B. floridanus* is found within small somatic cells lying under the basal lamina surrounding the ovariole; (iii) the bacterial endosymbionts rapidly infect all follicle cells and the transmission of the bacteria exclusively from follicle cells into the determined oocytes begins before the dOs enter the vitellarium; (iv) nurse cells are never infected by the bacteria; (v) during growth of the oocyte the endosymbionts are continuously transmitted into the oocyte, while the follicle cells are increasingly depleted of *Blochmannia*; (vi) during further growth the oocyte remains the only cell infected with bacteria, which are eventually located at the posterior pole of the egg before it is laid. In addition, the data suggest that *B. floridanus* may be transferred from follicle cells into the oocytes via regular exocytosis-endocytosis mechanisms. Finally, like in the midgut tissue, the gene expression data indicate a down-modulation of immune gene expression in the ovaries, which may support tolerance of the bacterial endosymbionts by the host within this tissue. The early infection of oocytes by the endosymbionts secures their vertical transmission in *C. floridanus* and thus the following ontogeny of the ants, which have been shown to be dependent on *Blochmannia* (Feldhaar et al., 2007; Stoll et al., 2010).

Some important questions are still unsolved, for example, where the endosymbionts infiltrating the ovaries are coming from. In a previous study, Hecht (1923) provided some insights regarding this question. He focussed on embryogenesis of the closely related ant *C. ligniperdus* and observed the translocation of the bacterial endosymbionts into primary bacteriocytes at the posterior pole of the egg in the course of cleavage division. During the formation of the blastoderm syncytium these primary bacteriocytes form the midgut together with endodermal cells. Additionally, endosymbionts get into large cells which will be enclosed by the embryonal band. During segmentation processes these endosymbiont harbouring cells are located between midgut and posterior pole of the embryo, the segment where ovary formation will take place (Hecht, 1923). Whether these early observations hold the key to understand the full cycle of vertical transmission of *Blochmannia* will be a task of future research.

Acknowledgements

We would like to thank Georg Krohne, Claudia Gehring as well as Daniela Bunsen of the Division of Electron Microscopy (Biocentre of the University of Würzburg) for valuable discussions and practical advice. We also would like to thank Annette Laudahn, Flavio Roces and Wolfgang Rössler of the Department of Zoology II of the Biocenter for help with animal breeding and husbandry. We thank Suvagata Roy Chowdhury for critically reading the manuscript. We gratefully acknowledge funding of this work by the German Research Foundation (DFG-GR1243/8-1).

Appendix A. Supplementary data

Supplementary data related to this article can be found at http://dx.doi.org/10.1016/j.asd.2016.09.004.

References

Aggrawal, K., Silverman, N., 2007. Peptidoglycan recognition in *Drosophila*. Biochem. Soc. Trans. 35, 1496–1500.

Asrat, S., de Jesus, D.A., Hempstead, A.D., Ramabhadran, V., Isberg, R.R., 2014. Bacterial pathogen manipulation of host membrane trafficking. Annu. Rev. Cell Dev. Biol. 30, 79–109.

Balmand, S., Lohs, C., Aksoy, S., Heddi, A., 2013. Tissue distribution and transmission routes for the tsetse fly endosymbionts. J. Invertebr. Pathol 112 (Suppl. l), S116–S122.

Baumann, P., 2005. Biology of bacteriocyte-associated endosymbionts of plant sap-sucking insects. Annu. Rev. Microbiol. 59, 155–189.

Blochmann, F., 1882. Über das Vorkommen bakterienähnlicher Gebilde in den Geweben und Eiern verschiedener Insekten. Zbl. Bakt. 11, 234–240.

Buchner, P., 1918. Vergleichende Eistudien. I. die akzessorischen Kerne des Hymenoptereneies. Arch. Mikrosk. Anat. II 91, 70–88.

Buchner, P., 1965. Endosymbiosis of Animals with Plant Microorganisms. Interscience, New York.

Dale, C., Moran, N.A., 2006. Molecular interactions between bacterial symbionts and their hosts. Cell 126, 453–465.

Doherty, G.J., McMahon, H.T., 2009. Mechanisms of endocytosis. Annu. Rev. Biochem. 78, 857–902.

Dunbar, H.E., Wilson, A.C.C., Ferguson, N.R., Moran, N.A., 2007. Aphid thermal tolerance is governed by a point mutation in bacterial symbionts. PLoS Biol. 5, 1006–1015.

Endler, A., Liebig, J., Schmitt, T., Parker, J.E., Jones, G.R., Schreier, P., Holldobler, B., 2004. Surface hydrocarbons of queen eggs regulate worker reproduction in a social insect. Proc. Natl. Acad. Sci. U. S. A. 101, 2945–2950.

Feldhaar, H., 2011. Bacterial symbionts as mediators of ecologically important traits of insect hosts. Ecol. Entomol. 36, 533–543.

Feldhaar, H., Gross, R., 2009. Insects as hosts for mutualistic bacteria. Int. J. Med. Microbiol. 299, 1–8.

Feldhaar, H., Straka, J., Krischke, M., Berthold, K., Stoll, S., Mueller, M.J., Gross, R., 2007. Nutritional upgrading for omnivorous carpenter ants by the endosymbiont *Blochmannia*. BMC Biol. 5, 48.

Fleig, R., 1995. Role of the follicle cells for yolk uptake in ovarian follicles of the honey bee *Apis mellifera* L. (Hymenoptera : Apidae). Int. J. Insect Morphol. Embryol 24, 427–433.

Gil, R., Silva, F.J., Zientz, E., Delmotte, F., Gonzalez-Candelas, F., Latorre, A., Rausell, C., Kamerbeek, J., Gadau, J., Holldobler, B., van Ham, R.C., Gross, R., Moya, A., 2003. The genome sequence of *Blochmannia floridanus*: comparative analysis of reduced genomes. Proc. Natl. Acad. Sci. U. S. A. 100, 9388–9393.

Gupta, S.K., Kupper, M., Ratzka, C., Feldhaar, H., Vilcinskas, A., Gross, R., Dandekar, T., Forster, F., 2015. Scrutinizing the immune defence inventory of *Camponotus floridanus* applying total transcriptome sequencing. BMC Genomics 16, 540.

Hecht, O., 1923. Embryonalentwicklung und Symbiose bei *Camponotus ligniperda*. Z. wiss. Zool. 122, 173–204.

Hybiske, K., Stephens, R.S., 2008. Exit strategies of intracellular pathogens. Nature Rev. Microbiol. 6, 99–110.

Jaglarz, M.K., Kloc, M., Bilinski, S.M., 2008. Accessory nuclei in insect oogenesis: in search of the function of enigmatic organelles. Int. J. Dev. Biol. 52, 179–185.

Kaltenpoth, M., 2009. Actinobacteria as mutualists: general healthcare for insects? Trends Microbiol. 17, 529–535.

Khila, A., Abouheif, E., 2008. Reproductive constraint is a developmental mechanism that maintains social harmony in advanced ant societies. Proc. Natl. Acad. Sci. U. S. A. 105, 17884–17889.

Klasson, L., Andersson, S.G., 2010. Research on small genomes: Implications for synthetic biology. BioEssays News Rev. Mol. Cell. Dev. Biol. 32, 288–295.

Klein, A., Schrader, L., Gil, R., Manzano-Marin, A., Florez, L., Wheeler, D., Werren, J.H., Latorre, A., Heinze, J., Kaltenpoth, M., Moya, A., Oettler, J., 2016. A novel intracellular mutualistic bacterium in the invasive ant *Cardiocondyla obscurior*. ISME J. 10, 376–388.

Kobialka, M., Michalik, A., Walczak, M., Junkiert, L., Szklarzewicz, T., 2015. *Sulcia* symbiont of the leafhopper *Macrosteles laevis* (Ribaut, 1927) (Insecta, Hemiptera, Cicadellidae: Deltocephalinae) harbors *Arsenophonus* bacteria. Protoplasma 253, 903–912.

Koch, A., 1960. Intracellular symbiosis in insects. Annu. Rev. Microbiol. 14, 121–140.

Koga, R., Meng, X.Y., Tsuchida, T., Fukatsu, T., 2012. Cellular mechanism for selective vertical transmission of an obligate insect symbiont at the bacteriocyte-embryo interface. Proc. Natl. Acad. Sci. U. S. A. 109, E1230–E1237.

Koressaar, T., Remm, M., 2007. Enhancements and modifications of primer design program Primer3. Bioinformatics 23, 1289–1291.

Kremer, J.R., Mastronarde, D.N., McIntosh, J.R., 1996. Computer visualization of three-dimensional image data using IMOD. J. Struct. Biol. 116, 71–76.

Livak, K.J., Schmittgen, T.D., 2001. Analysis of relative gene expression data using real-time quantitative PCR and the 2(-Delta Delta C(T)) Method. Methods 25, 402–408.

Login, F.H., Balmand, S., Vallier, A., Vincent-Monegat, C., Vigneron, A., Weiss-Gayet, M., Rochat, D., Heddi, A., 2011. Antimicrobial peptides keep insect endosymbionts under control. Science 334, 362–365.

Mastronarde, D.N., 2005. Automated electron microscope tomography using robust prediction of specimen movements. J. Struct. Biol. 152, 36–51.

Matsuura, Y., Kikuchi, Y., Hosokawa, T., Koga, R., Meng, X.Y., Kamagata, Y., Nikoh, N., Fukatsu, T., 2012a. Evolution of symbiotic organs and endosymbionts in lygaeid stinkbugs. ISME J. 6, 397–409.

Matsuura, Y., Kikuchi, Y., Meng, X.Y., Koga, R., Fukatsu, T., 2012b. Novel clade of alphaproteobacterial endosymbionts associated with stinkbugs and other arthropods. Appl. Environ. Microbiol. 78, 4149–4156.

McCutcheon, J.P., Moran, N.A., 2012. Extreme genome reduction in symbiotic bacteria. Nature reviews. Microbiology 10, 13–26.

Michel, T., Reichhart, J.M., Hoffmann, J.A., Royet, J., 2001. *Drosophila* Toll is activated by Gram-positive bacteria through a circulating peptidoglycan recognition protein. Nature 414, 756–759.

Nogge, G., 1981. Significance of symbionts for the maintenance of an optimal nutritional state for successful reproduction in hematophagous arthropods. Parasitology 82, 101–104.

Oliver, K.M., Degnan, P.H., Burke, G.R., Moran, N.A., 2010. Facultative symbionts in aphids and the horizontal transfer of ecologically important traits. Annu. Rev. Entomol. 55, 247–266.

Ratzka, C., Gross, R., Feldhaar, H., 2012. Endosymbiont tolerance and control within insect hosts. Insects 3, 553–572.

Ratzka, C., Gross, R., Feldhaar, H., 2013. Gene expression analysis of the endosymbiont-bearing midgut tissue during ontogeny of the carpenter ant *Camponotus floridanus*. J. Insect Physiology 59, 611–623.

Ratzka, C., Liang, C., Dandekar, T., Gross, R., Feldhaar, H., 2011. Immune response of the ant *Camponotus floridanus* against pathogens and its obligate mutualistic endosymbiont. Insect Biochem. Mol. Biol. 41, 529–536.

Reynolds, E.S., 1963. The use of lead citrate at high pH as an electron-opaque stain in electron microscopy. J. Cell Biol. 17, 208–212.

Riddell, C., Adams, S., Schmid-Hempel, P., Mallon, E.B., 2009. Differential expression of immune defences is associated with specific host-parasite interactions in insects. PloS One 4, e7621.

Romanelli, D., Casati, B., Franzetti, E., Tettamanti, G., 2014. A molecular view of autophagy in Lepidoptera. BioMed Res. Int. 2014, 902315.

Russell, J.A., Latorre, A., Sabater-Munoz, B., Moya, A., Moran, N.A., 2003. Side-stepping secondary symbionts: widespread horizontal transfer across and beyond the Aphidoidea. Mol. Ecol. 12, 1061–1075.

Sacchi, L., Grigolo, A., Mazzini, M., Bigliardi, E., Baccetti, B., Laudani, U., 1988. Symbionts in the oocytes of *Blattella germanica* (L.) (Dictyoptera: Blattellidae): their mode of transmission. Int. J. Insect Morphol. Embryol 17, 437–446.

Sauer, C., Dudaczek, D., Hölldobler, B., Gross, R., 2002. Tissue localization of the endosymbiotic bacterium "*Candidatus* Blochmannia floridanus" in adults and larvae of the carpenter ant *Camponotus floridanus*. Appl. Environ. Microbiol. 68, 4187–4193.

Schröder, D., Deppisch, H., Obermayer, M., Krohne, G., Stackebrandt, E., Hölldobler, B., Goebel, W., Gross, R., 1996. Intracellular endosymbiotic bacteria of *Camponotus* species (carpenter ants): systematics, evolution and ultrastructural characterization. Mol. Microbiol. 21, 479–489.

Steiner, H., 2004. Peptidoglycan recognition proteins: on and off switches for innate immunity. Immunol. Rev. 198, 83–96.

Stoll, S., Feldhaar, H., Fraunholz, M.J., Gross, R., 2010. Bacteriocyte dynamics during development of a holometabolous insect, the carpenter ant *Camponotus floridanus*. BMC Microbiol. 10, 308.

Swiatoniowska, M., Ogorzalek, A., Golas, A., Michalik, A., Szklarzewicz, T., 2013. Ultrastructure, distribution, and transovarial transmission of symbiotic microorganisms in *Nysius ericae* and *Nithecus jacobaeae* (Heteroptera: Lygaeidae: Orsillinae). Protoplasma 250, 325–332.

Szklarzewicz, T., Kalandyk-Kolodziejczyk, M., Kot, M., Michalik, A., 2013. Ovary structure and transovarial transmission of endosymbiotic microorganisms in *Marchalina hellenica* (Insecta, Hemiptera, Coccomorpha: Marchalinidae). Acta Zool. 94, 184–192.

Untergasser, A., Cutcutache, I., Koressaar, T., Ye, J., Faircloth, B.C., Remm, M., Rozen, S.G., 2012. Primer3–new capabilities and interfaces. Nucleic Acids Res. 40, e115.

Zchori-Fein, E., Roush, R.T., Rosen, D., 1998. Distribution of parthenogenesis-inducing symbionts in ovaries and eggs of *Aphytis* (Hymentoptera: Aphelinidae). Curr. Microbiol. 36, 1–8.

Zientz, E., Dandekar, T., Gross, R., 2004. Metabolic interdependence of obligate intracellular bacteria and their insect hosts. Microbiol. Mol. Biol. Rev. 68, 745–770.